Article

India's photovoltaic potential amidst air pollution and land constraints

India's Photovoltaic Potential amidst Air Pollution and Land Constraints

Impacting Solar Photovoltaic

Reflected

Clouds

Aerosols

Diffuse

Direct

Hypothesis

- Solar radiation
- Human settlement
- Vegetation index

Datasets

Indian Power grids

Northern
Eastern
North Eastern
Western
Southern

Region of Interest

Radiation 2001-18

AOD 2001-18

Cld Frac 2001-18

2017 2015 2013 2011 2009 2007 2005 2003 2001

Trend

Radiation

Aerosol-impact

Cloud-impact

Dimming/Brightening

$Wm^{-2}yr^{-1}$

-0.5   0   0.5

Land constraints

High Solar radiation, Barren/Shrub land,
No human settlement, Not over dense vegetations

Dimming/Brightening: Role of aerosols & clouds

Solar park

TGA
Utilizable
SPV
SPV:Aerosol-impact Avoided

North South West East N-East

Northern
Southern
Western
Eastern
N-Eastern

TGA Utilizable SPV SPV: Aerosol-impact Avoided

India
Dimming zones
N-East
East
West
South
North

Brightening zones

Aerosol & Cloud (Dim)
Aerosol only (Dim)
Cloud only (Dim)
Cloud only (Bright)

% Landmass

-30 -28 -26 -24 -22 -20 -18 -16 -14 -12 -10 -8 -6 -4 -2 0 2

Sushovan Ghosh,
Alok Kumar, Dilip
Ganguly, Sagnik
Dey

Sushovan.Ghosh@cas.iitd.ac.in

Highlights

A persistent dimming
prevailed over ~90% of the
Indian landmass during
2001–2018

Role of aerosols dominates
over clouds in modulating
observed trends in
irradiances

29% of the Indian region
can be utilized for solar
photovoltaic (SPV)

Alleviating aerosol burden
will make an additional 8%
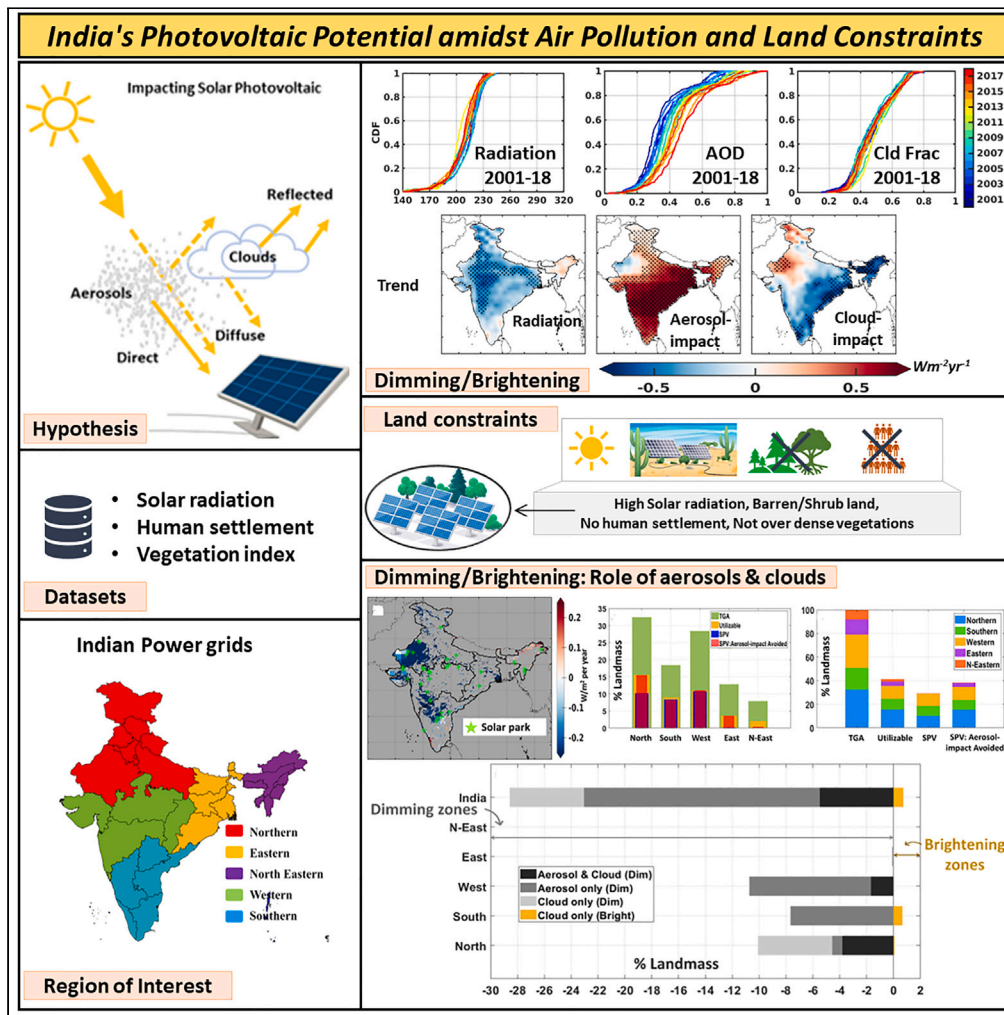area suitable for effective
SPV

iScience

Article

India's photovoltaic potential amidst air pollution and land constraints

Sushovan Ghosh,[1,4,*] Alok Kumar,[1] Dilip Ganguly,[1] and Sagnik Dey[1,2,3]

SUMMARY

India aims for ambitious solar energy goal to fulfill its climate commitment but there are limited studies on solar resource assessment considering both environmental and land availability constraints. The present work attempts to address this issue using satellite-derived air pollution, radiation, and land use data over the Indian region. Surface insolation over India has been decreasing at a rate of -0.29 ± 0.19 Wm^{-2} y^{-1} between 2001 and 2018. Solar resources over nearly 98%, 40%, and 39% of the Indian landmass are significantly impacted by aerosols, clouds, and both aerosols and clouds respectively. Only 29.3% of the Indian landmass is presently suitable for effective solar photovoltaic harnessing, but this is further declining by -0.21% annually, causing a presumptive loss of 50 GW solar potential, translating 75 TWh power generation. Lowering two decades of aerosol burden can make 8% additional landmass apt for photovoltaic use. Alleviating aerosol-induced dimming can fast-track India's solar energy expansion.

INTRODUCTION

Over the last two decades, solar photovoltaic (SPV) energy is growing prodigiously across the globe. In fact, India ranks fifth in the world in overall capacity building[1] and accounts for ~7% of the total global capacity.[2] Solar radiation, the prime factor for SPV generation, is often presumed to be constant for multiple years but many studies reported discernible multi-decadal variations. The changes in external forcing at the top of the atmosphere and/or internal forcing within the Earth's atmosphere alter the incoming radiation reaching the surface. Also, most of the earlier reports stressed the later factors and pointed out the roles of aerosols and clouds in observed multi-decadal variation referred to as 'dimming' and 'brightening' (i.e., decreasing or increasing trend in global horizontal irradiance, GHI respectively).

Prior studies have explicated a widespread decrease in shortwave radiation reaching the surface over land during the early 1990s.[3–5] A global study using long-term satellite data has shown the dimming effect until 1990, but an overall brightening tendency at a rate of 0.16 Wm^{-2} y^{-1} from 1983 to 2001.[6] Unlike a global transition from dimming to brightening, an unabated dimming continued in South Asia, particularly in the Indian sub-continents.[5,7] Many studies suggested that though clouds are the main modulator of short-term (within a day) fluctuations in surface solar radiation, most of these long-term (months to years) changes are driven by the changes in atmospheric aerosols emitted from anthropogenic sources.[7–12]

India has experienced a persistent dimming at a rate of -0.86 Wm^{-2} y^{-1} for the period of 1981–2004, with a more drastic decline during the later period of 1991–2000.[13] A slowdown of the prolonged dimming over the Indian landmass has been presented using a 40-year ground station dataset (1971–2010). It has showed a continuous dimming of -0.6 Wm^{-2} y^{-1} during 1971–2000 followed by a relatively mild dimming of -0.2 Wm^{-2} y^{-1} during 2000–2010. The patterns of the dimming/brightening are reported to be station-dependent and controlled by local to regional sources and meteorology.

In recent decades, investments in the solar energy industry are blooming in regions of a rapidly growing economy with a high level of particulate matter pollution, such as China, India, and the Middle East.[1,2] Renewable solar energy in India has been expanding since the introduction of the Jawaharlal Nehru National Solar Mission (JNNSM 2010). Additionally, India has set an ambitious solar renewable installation target of 100 GW by 2022.[14] Therefore, a deeper understanding of potential changes in surface solar irradiance and its ramifications toward the growing PV sectors in India (and elsewhere) is vital. Further, it demands appropriate resource mapping for the deployment of solar renewable at a national scale. This can be done by selecting appropriate sites based on the available GHI, proper land type, ease of transportation, accessibility of electrical grid-transmission lines, and the environmental factors that may debar the GHI.[15–17]

Geographical information system (GIS) are commonly used in solar renewable energy mapping.[18,19] In recent years, the GIS-based approaches are often combined with multi-criteria decision methods (MCDM) and or analytical hierarchy process (AHP).[20] These techniques are widely applied in various parts of the US,[21] Africa,[22,23] Europe,[24] Middle East,[25] and South Asia.[26–29] Most GIS-based resource mapping studies did not examine the interannual variability of GHI,[28] which is crucial for better financing of solar renewable energy,[30] having a typical

[1]Centre for Atmospheric Sciences, Indian Institute of Technology Delhi, New Delhi 110016, India
[2]Arun Duggal Centre of Excellence for Research in Climate Change and Air Pollution, Indian Institute of Technology Delhi, New Delhi 110016, India
[3]School of Public Policy, Indian Institute of Technology Delhi, New Delhi 110016, India
[4]Lead contact
*Correspondence: Sushovan.Ghosh@cas.iitd.ac.in
https://doi.org/10.1016/j.isci.2023.107856

Table 1. Climatological statistics of variant radiation fluxes from 2001 to 2018 over Indian landmass

Variables (Wm^{-2}) mean± stddev		Annual		DJF		MAM		JJA		SON	
All-Sky		209 ± 18		207 ± 32		260 ± 29		203 ± 31		195 ± 14	
Direct-All	Diffuse-All	90 ± 20	120 ± 10	86 ± 23	91 ± 23	130 ± 38	130 ± 38	51 ± 26	152 ± 26	91 ± 21	104 ± 21
Clear-Sky		256 ± 14		201 ± 24		295 ± 15		295 ± 22		233 ± 16	
Direct-Clear	Diffuse-Clear	166 ± 24	90 ± 12	140 ± 25	61 ± 25	199 ± 27	95 ± 27	173 ± 37	122 ± 37	153 ± 22	79 ± 22
NAER-Sky		233 ± 19		199 ± 35		287 ± 31		227 ± 34		218 ± 17	
Direct-NAER	Diffuse-NAER	137 ± 34	96 ± 20	126 ± 33	73 ± 33	193 ± 57	94 ± 57	88 ± 46	139 ± 47	140 ± 35	77 ± 34
Aerosol-Impact		24 ± 8		22 ± 9		27 ± 8		24 ± 8		22 ± 8	
Cloud-Impact		47 ± 20		24 ± 19		35 ± 30		91 ± 27		37 ± 17	
% Landmass (Aerosol-Impact>Cloud-Impact)		16%		71%		67%		5%		29%	

The percentage landmass shows the area where aerosol-impact exceeded the cloud-impact.

lifespan of 25–30 years. Earlier studies reported the aerosol impact on regional and global photovoltaic and concentrated solar re-sources.[31–35] In China, CSP potential decreased by 13% from 1961 to 2015 and increased by 16% when direct radiation returned to 1960s level.[12] In India, Dumka et al., 2021, 2022 pointed out the substantial impact on Indian solar power due to aerosol and cloud attenuation.[36,37] Further, Ghosh et al. 2022 showed that India lost 29% of its GHI potential due to aerosol loading between 2001 and 2018. These estimates did not consider the appropriate land type for SPV installations.[38] Additionally, the relative role of aerosols and clouds on the recent dimming and brightening of GHI in India is still being debated.

The dimming/brightening over India stated in previous studies are decades old and rely overwhelmingly on observations from urban sta-tions.[7,13,39] Since shrublands, barren areas, and arid regions are preferred for extensive SPV installation, the earlier studies have suffered from inadequate geographical representation and outdated evaluations of national-level solar resources. Further, the substantial growth in Indian solar energy underscores the importance of precise, up-to-date resource assessments considering accurate mapping of GHI and associated influencing factors.[15–17] The present investigation endeavors to tackle the stated issues. Moreover, earlier station-based studies are restricted to the trends of solar radiation, but its consequence toward the photovoltaic solar potential and SPV generation considering more likely land criteria, still need to be studied.

Here, we examine how solar irradiance over India has changed in recent decades and disentangle the relative roles of aerosols and clouds on observed trends during the satellite era using NASA's Clouds and the Earth's Radiant Energy System (CERES) data over the Indian region (6–38° N, 65–98° E).[40] This dataset provides computed surface, and profile radiant fluxes at different atmospheric states such as clear-sky (CS, including aerosol, no clouds), all-sky-no-aerosol (NAER, sky with 'no aerosol,' include clouds), and all-sky (AS, which consists of both aerosol and cloud, a better representation of the real atmosphere) conditions (see Table S1). These different radiation products are previously used to estimate the aerosol and cloud impact on solar energy generations.[31,35,38]

We presume that extinction linked with dimming and brightening can be better unveiled by considering direct and diffuse components of the various radiations. In addition, we assess the effect of dimming and/or brightening trends on India's photovoltaic solar energy resources and its generations. This has been done by identifying probable land availability and human settlement involvements using the combination of Moderate Resolution Imaging Spectroradiometer Normalized Difference Vegetation Index[41] (MODIS NDVI, 2015) and Global Human Set-tlement Layer (GHSL) data[42] (European Commission's GHSL, 2014). Further, we distinguish key regions (and the existing solar parks) within the Indian landmass that are sensitive to either aerosols or clouds linked with the observed trend.

There are studies on GIS-based resource mapping and an increasing number evidence on global dimming and brightening, but very limited studies on dimming and brightening effects on solar resource assessments.[12,30] Therefore, the current work is an attempt to fill this gap by assessing SPV resource for India in view of recent dimming and brightening with most plausible land use criteria using satellite observations.

RESULTS AND DISCUSSION

Surface dimming and brightening over India

India is endowed with an abundant amount of solar energy throughout the year, with ~300 sunny and clear-sky days annually[38,43,44] over the potentially high solar power regions. From 2001 to 2018, the Indian landmass has received an annual average irradiance of 209 ± 18 Wm^{-2} (5.0 ± 0.43 kWhm^{-2}d^{-1}) (Table 1). But, during the last two decades, persistent dimming has continued almost everywhere across the Indian region.[7] We find that 91% of its landmass is experiencing a dimming effect in all-sky radiation, with an average declining rate of −0.29 ± 0.19 Wm^{-2}y^{-1}. Compared to the surface radiation of the first decade of the 21st century (2001–2009), India has experienced a notable decline in all-sky radiation in the current decade (here, 2010–18), leading to an additional 13% of its landmass facing depleting trend (Figures 1 and S1; Table S2).
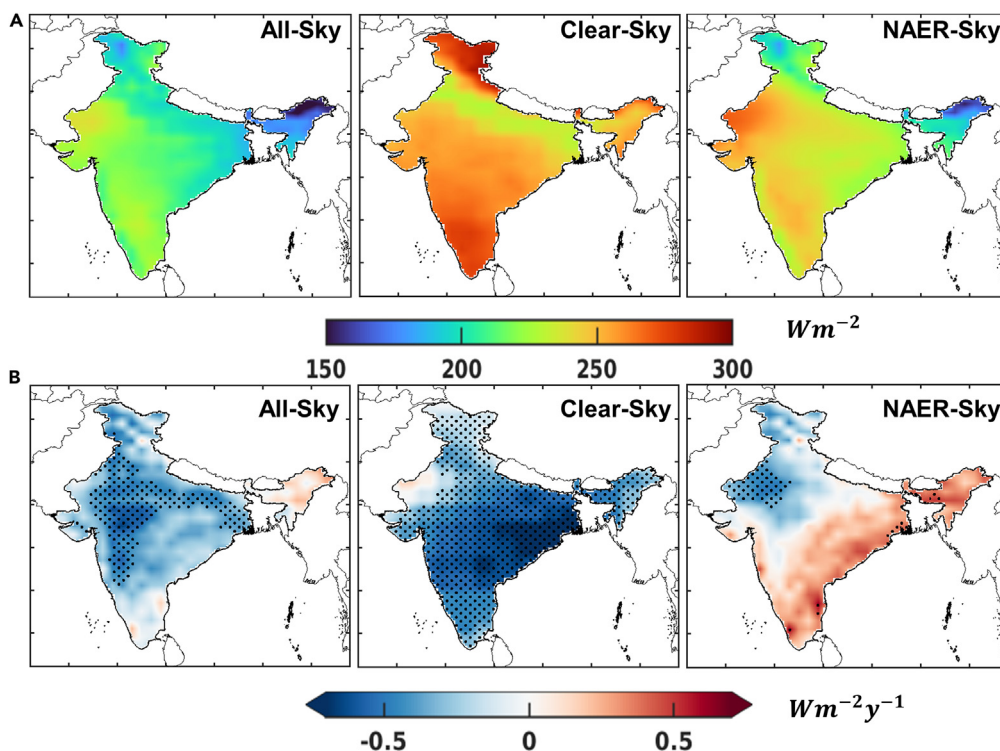
Figure 1. The eighteen-year (2001–18) climatology and trends of All-Sky, Clear-Sky, and No-Aerosol-Sky (NAER) surface radiation over India
(A) The climatology (in Wm^{-2}).
(B) Spatial trends (in Wm^{-2} y^{-1}) of the above surface fluxes during the period. The stipple in (B) shows the 95% significance level based on Student's *t* test.

The annual average diminishing rate in clear-sky irradiance (-0.46 ± 0.19 Wm^{-2}y^{-1}) is higher than the all-sky trends, while no-aerosol-sky irradiance exhibits a mild brightening effect (0.05 ± 0.26 Wm^{-2}y^{-1}) during the study period (Table 2). The clear-sky radiation mainly relies on aerosol loading, and no-aerosol-sky radiation is exclusively dependent on cloud cover and cloud characteristics. All-sky radiation can be interpreted as the manifestation of the combined impacts of aerosols and clouds (Figure S2). The combined trends in clear-sky and no-aerosol-sky radiations linked with the all-sky irradiance show that the GHI of 39% of the Indian landmass is negatively impacted by both aerosols and clouds, while 98% and 40% of regions are impacted individually by the direct effect of aerosols and clouds respectively (Figure S1).

The statistically significant dimming in clear-sky and all-sky radiation prevails across most parts of the Indo-Gangetic Plain (IGP) and some parts of western and central India in conjunction with high aerosol-loading.[45] In contrast, a brightening effect in all-sky radiation, in-line with the no-aerosol-sky radiation pattern, is observed over most parts of north-eastern India and a few regions on the southern coast. The Thar Desert in northwest India experiences a nominal brightening effect in clear-sky conditions while strong and statistically significant dimming in no-aerosol-sky radiation, causing a clement dimming tendency in all-sky irradiance. Likewise, the competing effect of brightening in no-aerosol-sky radiation and significant dimming in clear-sky radiation results in an overall mild dimming in all-sky irradiance across most parts of the Indian coastline (Figure 1B).

The seasonal analysis in GHI shows that India receives maximum insolation during pre-monsoon (Mar-May) followed by monsoon (Jun-Aug) and minimum during winter (Dec-Feb), with the highest intensity over western and southern India and lowest over the north-eastern regions (Table 1; Figure S3A).

The magnitude of the dimming trend (-0.38 ± 0.3 Wm^{-2}y^{-1}) is the highest during winter (prevails over ~87% of the landmass, Figure S1), followed by the monsoon, and is the lowest during pre-monsoon (-0.22 ± 0.27 Wm^{-2}y^{-1}) season. This agrees well with the observed trend reported in India during an earlier period from 1990 to 2006.[39] Typically, aerosols in winter and clouds during monsoon drive these variabilities (Figures S3B and S4; Table 2).

Recent trends in direct and diffuse radiation

The total radiation (here, all-sky/clear-sky/no-aerosol-sky) is composed of direct and diffuse parts. The spatiotemporal patterns in diffuse radiation over India are complex and inhomogeneous, while total irradiance is concomitant with direct radiation. Annually, the direct component of the total radiation is greater under clear-sky conditions (166 ± 24 Wm^{-2}) than it is under all-sky conditions (90 ± 20 Wm^{-2}). Likewise, the magnitude of diffuse radiation is highest under all-sky conditions (120 ± 10 Wm^{-2}) and lowest under clear-sky conditions (90 ± 20 Wm^{-2}). In addition, the direct irradiance is strongest in the north-west and south of India, while the diffuse radiation is most prominent along the coast

Table 2. Trend statistics of variant radiations, Aerosol Optical Depth (AOD), and cloud fraction from 2001 to 2018

Variables (2001-18) $mean \pm std\ dev$ (% Landmass experiencing[a,b])	Annual	DJF	MAM	JJA	SON
All-Sky[a] ($Wm^{-2}\ y^{-1}$)	-0.29 ± 0.19 (-91%)	-0.38 ± 0.36 (-87%)	-0.22 ± 0.26 (-82%)	-0.33 ± 0.36 (-83%)	-0.25 ± 0.38 (-72%)
Clear-Sky[a] ($Wm^{-2}\ y^{-1}$)	-0.46 ± 0.19 (-98%)	-0.57 ± 0.23 (-100%)	-0.39 ± 0.29 (-92%)	-0.39 ± 0.20 (-96%)	-0.51 ± 0.23 (-99%)
NAER-Sky[a] ($Wm^{-2}\ y^{-1}$)	0.05 ± 0.26 (-40%)	0.05 ± 0.33 (-44%)	0.11 ± 0.33 (-29%)	-0.17 ± 0.43 (-60%)	0.15 ± 0.38 (-35%)
Aerosol-Impact[b] ($Wm^{-2}\ y^{-1}$)	0.33 ± 0.20 (94%)	0.43 ± 0.20 (100%)	0.33 ± 0.32 (88%)	0.17 ± 0.15 (88%)	0.40 ± 0.21 (97%)
Cloud-Impact[b] ($Wm^{-2}\ y^{-1}$)	-0.17 ± 0.24 (25%)	-0.19 ± 0.26 (23%)	-0.17 ± 0.29 (19%)	-0.05 ± 0.42 (43%)	-0.26 ± 0.32 (26%)
AOD[b] (Unitless) per year or y^{-1}	0.009 ± 0.004 (97%)	0.01 ± 0.004 (100%)	0.007 ± 0.006 (87%)	0.0008 ± 0.005 (96%)	0.01 ± 0.005 (97%)
Cloud fraction[b] (Unitless, Scale: 1) per year or y^{-1}	0.0003 ± 0.001 (61%)	0.0009 ± 0.003 (60%)	0.00003 ± 0.002 (50%)	0.001 ± 0.003 (75%)	-0.0009 ± 0.002 (36%)

The negative sign signifies dimming, and the positive for brightening effect for All-sky, Clear-sky, and NAER-sky radiation, and the positive/negative sign in Aerosol-impact, Cloud-impact, AOD, and Cloud fraction signifies increasing/decreasing pattern over Indian landmass. The trends are statistically significant at 95% confidence level. DJF: December-February, MAM: March-May, JJA: June-August, SON: September-November.

[a]% Landmass experiencing: *indicates the percentage of Indian landmass where dimming prevails (decreasing trends of All-sky, Clear-sky, and NAER-sky).*

[b]% Landmass experiencing: indicates the percentage of Indian landmass where increasing trends prevails (Aerosol-impact, Cloud-impact, AOD, and Cloud fraction).

and in the Northeast India (see Table 1; Figure S5). These results suggest the dominant role of clouds relative to aerosols in modulating direct and diffuse radiation.

The annual-averaged trend in direct radiation under all-sky conditions shows that 71% of the Indian landmass experiences dimming effects in direct irradiance with an average depleting rate of $-0.20 \pm 0.40\ Wm^{-2}y^{-1}$ and is the highest over the IGP and south-west India. This decreasing tendency is in-line with the severe dimming trends in clear-sky irradiance ($-1.08 \pm 0.50\ Wm^{-2}y^{-1}$, dimming prevails over 97% of Indian landmass) but completely out-of-phase with the direct component of no-aerosol-sky irradiance's tendency ($0.47 \pm 0.67\ Wm^{-2}y^{-1}$, brightening prevails over 77% Indian landmass). On the other hand, under all-sky conditions, India suffers a faint dimming in diffuse radiation ($-0.08 \pm 0.31\ Wm^{-2}y^{-1}$, sustaining over 62% of its landmass) while an acute brightening continues in diffused clear-sky radiation ($0.63 \pm 0.33\ Wm^{-2}y^{-1}$, brightening prevails over 95% of its landmass) except over the Thar Desert in northwest India. The dimming effect of diffused no-aerosol-sky radiation ($-0.42 \pm 0.48\ Wm^{-2}y^{-1}$, sustaining over 82% of its landmass) offsets the brightening impact of diffused clear-sky radiation and results in a pale dimming in diffused all-sky irradiance (stated above, see Figure 2; Table S3).

The massive dimming trend in direct clear-sky radiation outweighs the brightening of no-aerosol-sky radiation (except in a few parts of the southern coastline), resulting in a mild dimming in direct all-sky irradiance. However, in Northeast India, the brightening tendency of direct no-aerosol-sky predominates over the dimming of direct clear-sky irradiance, while over the Thar Desert in northwest India, dimming of direct no-aerosol-sky irradiance offsets brightening of direct clear-sky radiation. Likewise, the dimming tendency of diffused no-aerosol-sky irradiance across the Indian coastline supersedes the brightening effect of clear-sky irradiance entails in a nominal dimming in diffused all-sky across the coastline (see Figure 2).

Recent trends in aerosol- and cloud-induced dimming and brightening

Aerosols and clouds both impair the incoming solar radiation reaching the surface. But the attenuation effect of clouds outweighs the aerosols. The annual average cloud impact ($47 \pm 20\ Wm^{-2}$) is almost twice that of aerosol impact ($24 \pm 8\ Wm^{-2}$). However, during the last eighteen-year (2001-18), 15% of the Indian landmass experiences more aerosol-induced impedance in surface flux as compared to the cloud impact. Moreover, as compared to the past decade (2001-09), in the recent decade (2010-18), an additional 2% aerosol-impacted area has been increased (see Table 1; Table S2).

Seasonal analysis shows that India suffers the highest impact of aerosols ($27 \pm 8\ Wm^{-2}$) during pre-monsoon due to staggering aerosol loading while cloud-induced radiation impairment ($91 \pm 27\ Wm^{-2}$) occurs during monsoon due prevalent cloud cover. The maximum aerosol effect is pervaded across the IGP and cloud-effect along the Indian coastline and northeast India (see Figure 3A; Table 1).

The annually averaged aerosol impact is increasing ($0.33 \pm 0.20\ Wm^{-2}y^{-1}$), and the cloud impact is decreasing ($-0.17 \pm 0.24\ Wm^{-2}y^{-1}$) (Table 2). This soaring trend in aerosol impact is sustaining almost ~94% of the Indian landmass and more intensified over the IGP and eastern coastline. However, there is a reducing tendency over the north-western Thar Desert. The trends in aerosols' loading ($0.009 \pm 0.004\ years^{-1}$
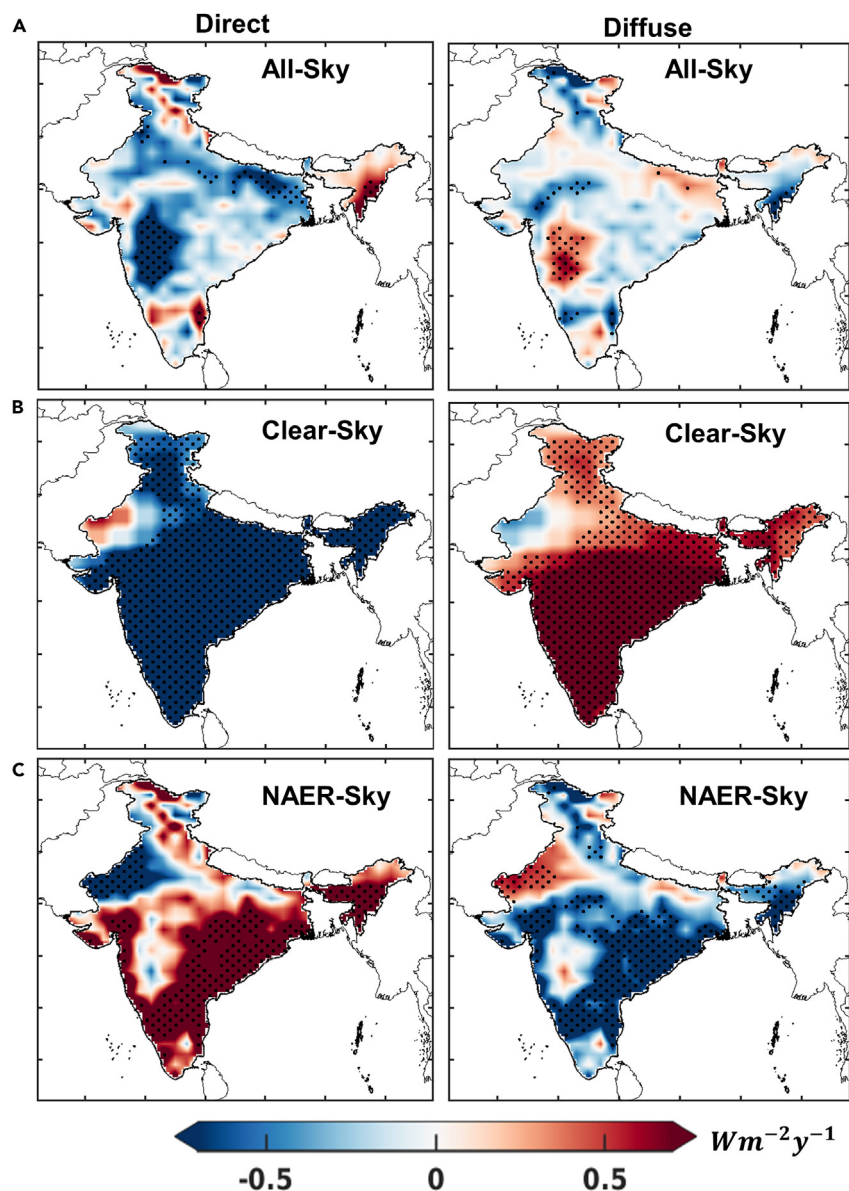
Figure 2. Spatial trends in Direct (left column) and Diffuse (right column) radiation of the variant surface fluxes from 2001 to 2018 (in Wm^{-2} y^{-1})
(A) All-Sky.
(B and C) (B) Clear-Sky and (C) NAER-Sky. The stipple in the above figure shows the 95% significance level based on Student's t test.

and escalating trends that prevail in 97% of the Indian landmass) mostly drive the intricacy of spatiotemporal patterns of aerosol-induced dimming and or brightening (see Figure 3B). The highest aerosol impact is observed during winter (Dec-Feb, 0.43 $\pm$ 0.20 Wm^{-2}y^{-1}, and prevails across the Indian landmass) followed by post-monsoon (Sep–Nov) and is in line with the rapidly increasing aerosol loading tendency during winter (0.01 $\pm$ 0.004 years^{-1} and increasing trends prevails across the Indian landmass). The observed aerosol impacts during the pre-monsoon period (April to early June) can be attributed to the presence of dust storms[46] across the Indo-Gangetic Plain. Furthermore, in the months of April-May and October-November, the aerosol influence can be linked to the forest fire[37] and agricultural residue burning[47] in various regions of northern, eastern, central, and northeastern India. The monsoon rain washes out aerosols, and hence the aerosol contribution to depleting surface fluxes is observed to be the lowest (see Table 2; Figures S4–S7).

On the other hand, annually, only 25% of the Indian landmass (mostly the north-western regions) suffers from the increasing tendency of cloud impact. The maximum influence of cloud impact on the depletion of surface flux (-0.05 ± 0.42 Wm^{-2}y^{-1}) is observed during monsoon in congruence with cloudiness tendency (0.001 $\pm$ 0.003 years^{-1}). However, there is a persisting year-round decreasing trend
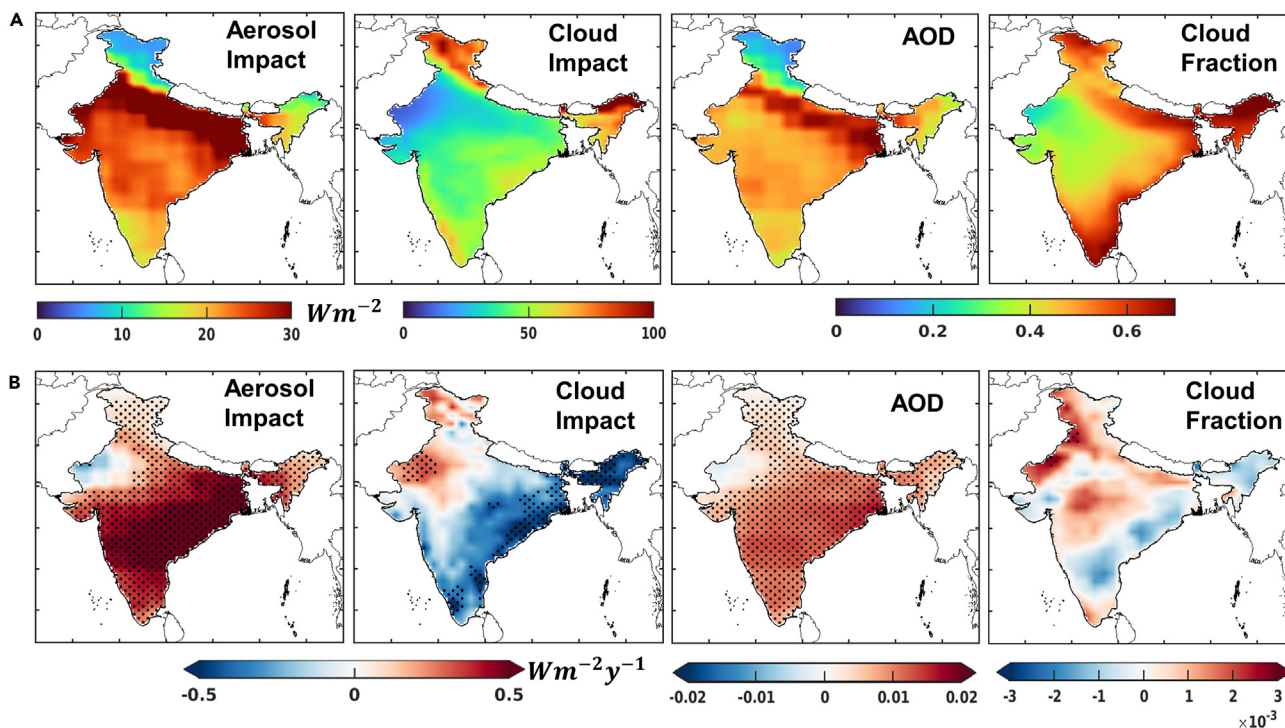
Figure 3. The eighteen-year (2001–2018) climatology and spatial trend over India landmass

(A) The climatology of Aerosol-impact (Wm^{-2}), Cloud-impact (Wm^{-2}), Aerosol Optical Depth (AOD), and Cloud fraction over India.

(B) Spatial trends of the above quantities during the period (in the same order). The stipple in (B) shows the 95% significance level based on Student's *t* test.

in cloud-influence along the Indian coastline and north-eastern region except the south-western coast during monsoon. This reducing tendency in cloud impact invites a brightening effect in no-aerosol-sky irradiance, in accordance with the decreasing trends in cloud fraction (see Table 2; Figures S4–S7).

Key regions over Indian landmass

The aerosol optical depth (AOD, a columnar integral of aerosols distributed within a column of air ranging from earth's surface to the top of the atmosphere) and total cloud fraction are the two most important factors governing aerosol and cloud impacts, respectively. Hence, their trends are critical for the trends in clear-sky and no-aerosol-sky irradiance, which ultimately gets manifested in the trend of all-sky radiation. In regions like the Thar Desert in northwest India, we find a decreasing trend in AOD, aerosol impact, and finally, the brightening tendency in clear-sky irradiance. The decomposition analysis using the Modern-Era Retrospective Analysis for Research and Applications, version 2 (MERRA2)[48,49] reveals that the AOD trend here is influenced mostly by the declining dust loading[50] (Figure S8). Conversely, the increasing trends in total cloud fraction, primarily governed by high-level clouds, cause dimming in no-aerosol-sky irradiance. The net result of these two competing effects is a moderate dimming in all-sky irradiance. If the current trend continues, the region will be more cloud sensitive. The increasing trends in high-level clouds in the north-western part are evident during the monsoon season as well (Figure S9).

On the contrary, along the Indian coastline and north-eastern region, the decreasing trends of total cloud fraction ramifies the brightening effect of no-aerosol-sky radiation. But, in the eastern IGP and along the coastline, the increasing aerosol loading[45] due to continual anthropogenic activities introduces a severe dimming trend in the clear-sky radiations and outweighs the brightening effect of no-aerosol-sky, fabricating the region more aerosol-sensitive and resulting in dimming in all-sky irradiance. However, in north-eastern regions, the no-aerosol-sky regulates the tendency of all-sky irradiance, shaping the region more cloud sensitive.

Assessing solar resources in India

Previous studies showed that 60% of the total geographic area (TGA) of India is exposed to more than 5 kWhm^{-2}d^{-1} of radiation (the threshold for effective utility-scale SPV generation).[38,51] But these estimates did not consider suitability of land criterion. Hence, the studies include a vast share of agricultural and forestry land which are not preferred for utility-scale SPV plants due to ecological preservations and environmental constraints. In this present study, we have identified probable land for ground-mounted large-scale to rooftop SPV installations based on NDVI and GHSL criteria (see STAR methods). This includes 41% of Indian TGA (spreading 15.5% over northern, 11% over western, 8.98% over southern, 3.6% over eastern and 2% over north-eastern power grids) and incorporates mostly desert, barren, scrubland, and

wasteland for ground-mounted set-up and rural to urban spaces for the rooftop installations (Figures 4A, 4B, 5A–5C, and S10). However, only 29.3% of the Indian TGA has been emerged as potential region for effective SPV generations (irradiance $\geq$ 5kWhm^{-2}d^{-1}). Most of these land-masses are located over western power grid (10.73%) followed by northern (10.15%), southern (8.36%) and lowest over the eastern grid (0.08%). Mainly the terrain suitability, human settlement and the available GHI govern this resource mapping. Moreover, the criterion finds that north-eastern power grid is not a preferred location for effective SPV installations (Figures 4A, 4B, 5E, and 5G). The geo-locations of the already existing Indian solar parks over our SPV potential landmass across the power grids establishes the credibility of our proposed land-criterion (see Table S4; Figures 5A–5G and S10). Additionally, the spatial distribution of the potential landmass for SPV installation is in good agreement with the recent study using Multi-criteria Analysis Planning Renewable Energy (MapRE) over India.[27] Further, our analysis finds that ~28.56% of the TGA are experiencing dimming at an average annual rate of -0.29 ± 0.11 Wm^{-2} y^{-1}. The eastern power grid suffers highest dimming (-0.43 ± 0.10 Wm^{-2}y^{-1}) followed by western (-0.37 ± 0.13 Wm^{-2} y^{-1}), northern (-0.28 ± 0.14 Wm^{-2} y^{-1}) and lowest over southern power grid (-0.16 ± 0.12 Wm^{-2} y^{-1}) (Figures 4C–4D and S11). The 5.5% of the TGA (spreading ~3.8% over northern, ~1.7% over western power grids) are encountering dimming due to increasing trends of both aerosol and cloud, while 18% of TGA experiences domi-nance in aerosol-impact (encompassing ~9% over western, ~8% over southern, and rest over northern and eastern power grids) and ~5.5% of TGA (mainly over northern power grid) faces prepotent cloud-impact. Further, ~0.7% of Indian TGA confronts brightening (spreading 0.66% over southern, rest over northern power grids) due to declining of cloud-impact only.

Dimming over western, southern, and eastern power-grids are mainly governed by staggering aerosol loading while northern power-grid is affected by both the aerosols and cloud. However, clouds play pivotal role in determine dimming over northern grid (Figures 4C–4D and S11). Further, we have found that the coverage of the potential hotspots (i.e., ~29.3% of Indian TGA) has been depleting at an annual rate of 0.21% y^{-1} during the last 18-year (2001-18) (Figure S12H). This is equivalent to the loss of at least 50 GW SPV potential (considering land use factor of 7.5 MWkm^{-2}),[27] which can generate at least 75 TWh of solar electricity annually (typically 1MW plant can produce 1.44 GWh on a mean year basis, see STAR methods). Precluding almost two decades of aerosol burden, results in increase in available GHI by 7–15% across the five regional power grids (Figure 4E). Further, India would have achieved 37% of its total landmass suitable for potential SPV set-up. Over-all, ~8% enhancement in SPV potential land (spreading ~5% over northern, ~3% over eastern and rest ~1% over western and north-eastern power grids, Figures 4, 5E–5I, and S13). Most of the potential states (mean available GHI $\geq$ 5kWhm^{-2}d^{-1}) are in southern, western, and in northern power grids, but none from eastern and north-eastern power grids. However, by avoiding the staggering aerosol burden, the na-tional capital region of Delhi (NCR-Delhi) in the northern grid, Bihar, Jharkhand, and West Bengal in the eastern grid, and Tripura, Mizoram, and Meghalaya in the north-eastern grid emerge to be the SPV potential states (Figures 5I–5l and S13). Earlier studies pointed out that the population's daily activities in the eastern and north-eastern power grid mainly depend on burning fossil fuel and biomass. Therefore, the clean air initiatives and renewable solar expansion will bring positive feedback toward sustainable livelihood.[52] Sikkim, one of the cleanest states, where mean exposed radiation is below the threshold, avoiding aerosol burden does not influence the SPV potentiality (Figure 5I).

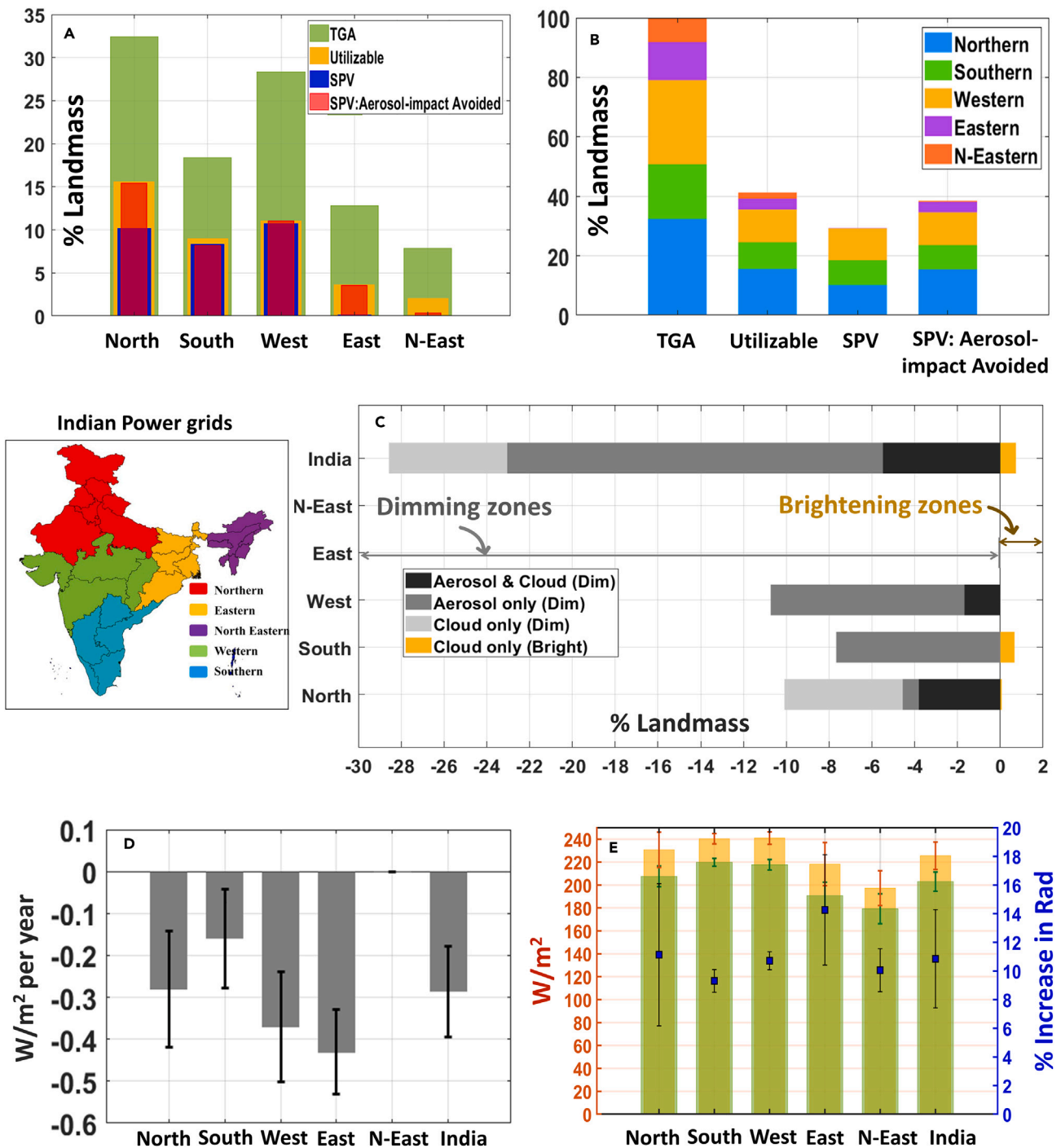### Effect of dimming/brightening to optimally tilted panel

In India, optimally tilted solar panels, either as a ground-mounted set-up or roof-top installation, are commonly used, and trackers are func-tional in very few plants (TATA Power Solar 2017 Track them down! Solar today July-September available at: www.tatapowersolar.com/wp-content/uploads/2018/01/02052435/Feature-Solar-Tracker.pdf). The annual average exposed radiation on ideally tilted fixed solar panel sur-faces is 305 $\pm$ 30 Wm^{-2} (~1.5 times more w.r.t. horizontal flat surface configurations) but declining at a rate of -0.59 ± 0.63 Wm^{-2}y^{-1} (~twice w.r.t. horizontal flat surface settings) which is equivalent to ~0.20% of the annual mean exposed radiation. This translates to a loss of ~100 GWh of generation annually (considering India's annual solar power generation of 50 TWh till 2019-20), equivalent to ~5 million USD (considering INR 3.85 kWh^{-1} (~0.052 USD kWh^{-1}) of consumption (STAR methods and Figure 6). Besides, by overcoming the last 18-year of aerosol burden, India would have realized a mean exposure of 385 $\pm$ 50 Wm^{-2} (~26% increase w.r.t. fixed-tilted GHI climatology), rendering 13 TWh surplus generation, equivalent to 675 million USD revenue (see Figure 6). The states across the Indo-Gangetic Plain (IGP), such as NCR-Delhi, Uttar Pradesh, Haryana, Punjab (in the northern power grid), and West Bengal, Bihar, and Jharkhand (in the eastern power grid), experience the highest benefits in radiation enhancement. Promoting "at least one solar city in each state" [https://www.livemint.com/news/india/pm-modi-calls-for-each-state-to-have-one-solar-city-11590659943808.html], along with the efforts to curb aerosol loading, will surely add heft to India's green energy credential and path toward the formation of a sustainable nation.
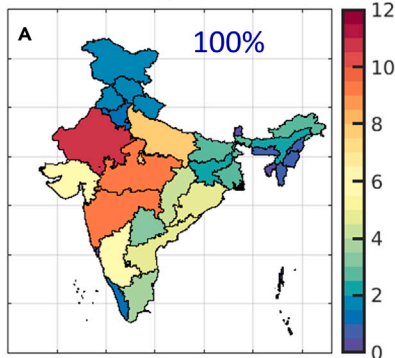
DISCUSSION

In the present work, we estimate the losses in surface irradiance in India due to aerosols and clouds and discuss the potential impacts on solar energy resources based on recent dimming and brightening trends and land availability. The variant radiation fluxes within this dataset pro-vides a unique scope to isolate the aerosols and cloud contributions in the observed trends. Recently, the CERES datasets for the same period (2001–18) have been validated against station-based observation over the Indian region and are not repeated here.

Our study reveals that India is experiencing an unabated dimming almost across its landmass with an average rate of -0.29 ± 0.19 Wm^{-2}y^{-1} during the study period. This finding is concomitant with the earlier reports carried out using station-based networks.[39] The increasing rate of dimming in clear-sky radiation, along with the overall brightening in no-aerosol-sky radiation, alludes to the dominant role of aerosols over clouds in modulating the dimming in all-sky irradiance.
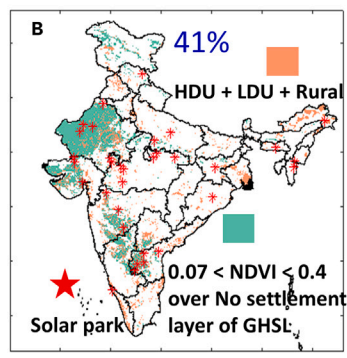
Annually, every 10% change in AOD can lead to a 22 Wm^{-2} change in aerosol-induced attenuation, and every 10% change in cloud fraction (scale of 1) can result in a 44 Wm^{-2} change in cloud-induced effects (Figure S14). Climatologically, the cloud impact has been dominant along
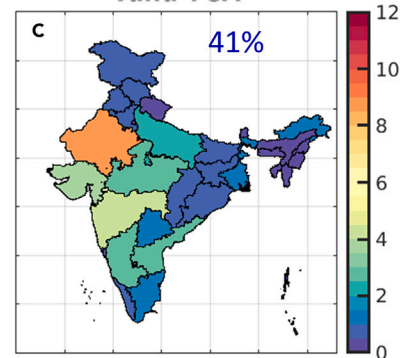
Figure 4. Solar photovoltaic potential across the Indian power-grids

(A) Power grid-wise distribution of percentage landmass concerning Total Geographical Area (TGA), Utilizable landmass, Solar Photovoltaic potential land (SPV) and Solar Photovoltaic potential land (SPV): avoiding aerosol induced losses.

(B) same as (A) but over entire Indian landmass.

(C) Distribution of percentage landmass concerning the role of individual aerosol, clouds, and both on the observed dimming/brightening over the power grids in India.

(D) Trends in GHI over the SPV potential regions across the power-grids and India. The vertical line refers standard deviation.

(E) GHI (light green), GHI: Avoiding aerosol impact (light orange) and percentage increase in radiation (blue square) over the power grids and India. The vertical lines with respective colors refer standard deviation.

A Total Geographic Area (%) contribution — 100%

B Utilizable land: SPV installations — 41% — HDU + LDU + Rural — 0.07 < NDVI < 0.4 over No settlement layer of GHSL — Solar park

C Utilizable land (%) contribution — 41%

D GHI Climatology 2001-18 (kWh m⁻² d⁻¹) — 41%
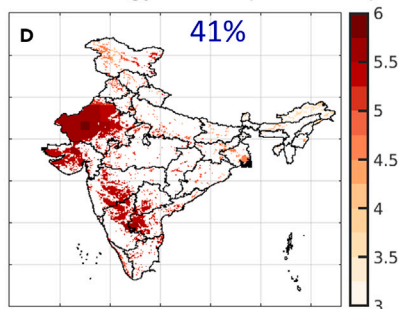
E GHI ≥ 5 kWh m⁻² d⁻¹: Climatology — 29%
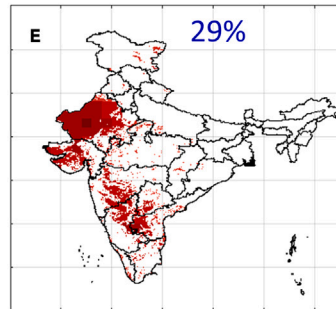
F GHI Climatology : Avoided aerosol impact — 37%
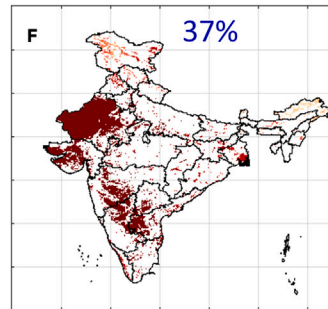
G SPV potential land (%) contribution — 29%
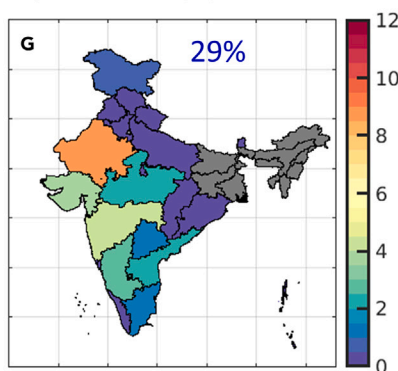
H SPV potential land: Avoided aerosol impact — 37%
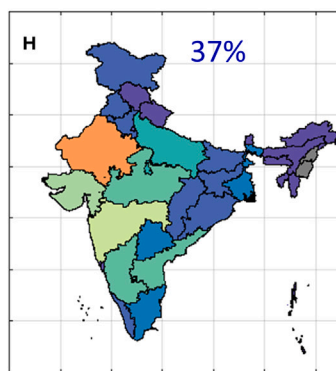
I Increase in SPV potential land (%) — 8%
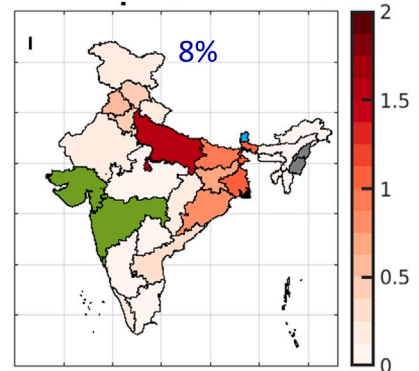
J GHI Climatology 2001-18 (kWh m⁻² d⁻¹) — 4.9 kWhm⁻²d⁻¹
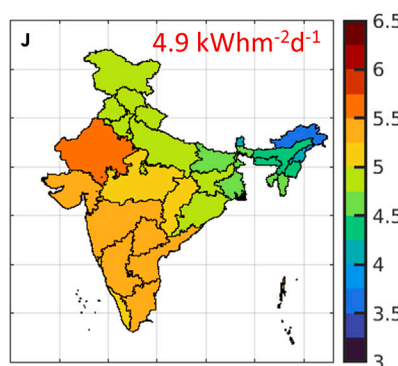
K GHI: Avoided aerosol impact (kWh m⁻² d⁻¹) — 5.4 kWhm⁻²d⁻¹
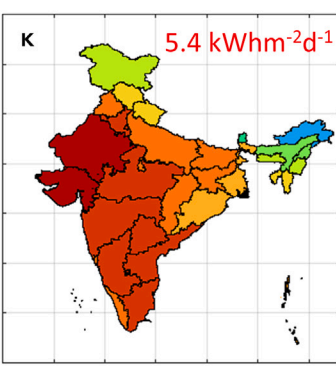
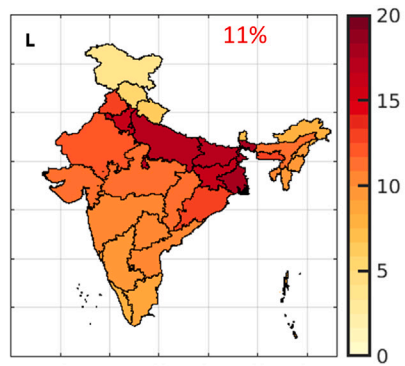**L** Increase in GHI (%) w.r.t. GHI climatology — 11%

Figure 5. Indian State and Union Territories (UTs) specific illustration of solar photovoltaic potential and Global Horizontal Irradiance (GHI) distributions

(A) Percentage contribution of each state toward the Total Geographical Area (TGA) of India.

(B) Probable utilizable land for roof-top and ground-mounted installations based on NDVI and GHSL criteria. GHSL includes High-Density Urban (HDU), Low-Density Urban (LDU), Rural, and No-settlement layers.

(C) Percentage contribution of each state toward utilizable land for SPV set-up.

(D–F) (D) GHI climatology, (E) GHI ($\geq$5kWh m^{-2} per day), (F) GHI: avoiding 18-year of aerosol burden over the probable utilizable land.

(G) Percentage contribution of each state toward SPV hotspots.

(H) Percentage contribution of each state toward SPV hotspots avoiding aerosol loading.

(I) Percentage contribution of each state toward SPV hotspots considering avoiding aerosol load and baseline scenario (obtained as (H) minus (G)). Dark gray in (G–I) Figures over the states indicates no availability of SPV potential area. Green color over states on (I) indicates all places within those states are SPV potential areas, and cyan over Sikkim on (I) indicates no change in SPV potentiality due to low GHI with very low aerosol loading. The blue color percentage in (A–I) is summative of the identified areas w.r.t. the TGA of India.

(J–L) (J) state-wise mean GHI, (K) state-wise mean GHI: avoiding aerosol burden, (L) Percentage increase in GHI w.r.t. mean GHI (baseline scenario). The red color on (J and K) is the all-India average GHI, and 11% in (L) is the all-India average increase in GHI considering avoiding aerosol load and baseline scenario (obtained as (K) minus (J) divided by (J)).

the Indian coastline, north-eastern regions, and lowest over the northwest Thar Desert. On the other hand, the aerosol impact is more prominent over the IGP, and its dominance gradually decreases in Peninsular India. However, during the last 18 years, cloud impact (modulated primarily by cloud fraction) has been decreasing along the Indian coastline and over northeast India. In contrast, aerosol impact (modulated primarily by AOD) is increasing everywhere except over the northwest Thar Desert. Furthermore, there is a notable increase in aerosol-induced dimming at forest fire hotspots[37] (i.e., over central Himalaya, north-east and central India) (Figure S15). Over the Thar Desert, the role of clouds (and specifically high-level clouds) outweighs the aerosol loading. If the current trend continues, then the existing solar parks over that region of Rajasthan will be more sensitive to changes in cloud characteristics (in response to global warming), even though they experience desert dust inherently. This demands further investigation using a modeling framework. On the other hand, over Northeast India, the brightening effect is synchronous with the decreasing cloud fraction.

Here, we address the issue pertaining to land scarcity by identifying probable land for harnessing solar energy based on the NDVI, GHSL, and irradiance criteria. This land includes barren, shrubland, desert, and other wasteland and considers 29.3% of the TGA of India as an SPV hotspot. Our proposed methodology for land availability criteria is unique and simple and reusable to any region of similar essence. The use of human settlement spaces such as HDU, LDU, and rural areas promote the various clean energy schemes of Government of India (GoI) such as "solar city," "rural electrification," and "agro-photovoltaics." Reducing aerosol burden by meeting clean air targets set by the GoI is expected to enhance solar resources and generations. A study can be designed to target various sources of particulate matter to mitigate the impact of aerosols originating from multiple sources and reduce solar energy production.

Our analysis reveals that alleviating the aerosol-induced dimming over the Indian region will accelerate its growth in solar renewable energy in the coming years. This will further encourage the nation's pledge toward clean affordable energy to every individual. We recommend that policymakers, planners, and investors should consider the impact of aerosols, clouds, and the dimming and brightening effect on solar resource assessment while conducting solar energy expansion exercises in India (or elsewhere).

Limitations of the study

Unlike earlier estimates where no land use criteria were involved in determining the impact of air pollution and dimming or brightening on SPV resources, our analysis provides precise and first-hand assessment to date. However, we do not consider the cost pertaining to the infrastructure development of solar installations at the identified locations. Also, we only investigate the direct effect as an aerosol impact and do not include aerosol-induced cloud impact;[53,54] there could be additional benefits or losses in solar energy due to changes in aerosol loadings in the future. This aspect and the influence of cloud microphysical properties on cloud impact need to be investigated in a model-based setup.

STAR★METHODS

Detailed methods are provided in the online version of this paper and include the following:

- KEY RESOURCES TABLE
- RESOURCE AVAILABILITY
  - Lead contact
  - Materials availability
  - Data and code availability
- METHOD DETAILS
  - Solar radiation datasets
  - Cloud datasets
  - NDVI and GHSL datasets
  - Solar energy capacity and generation datasets
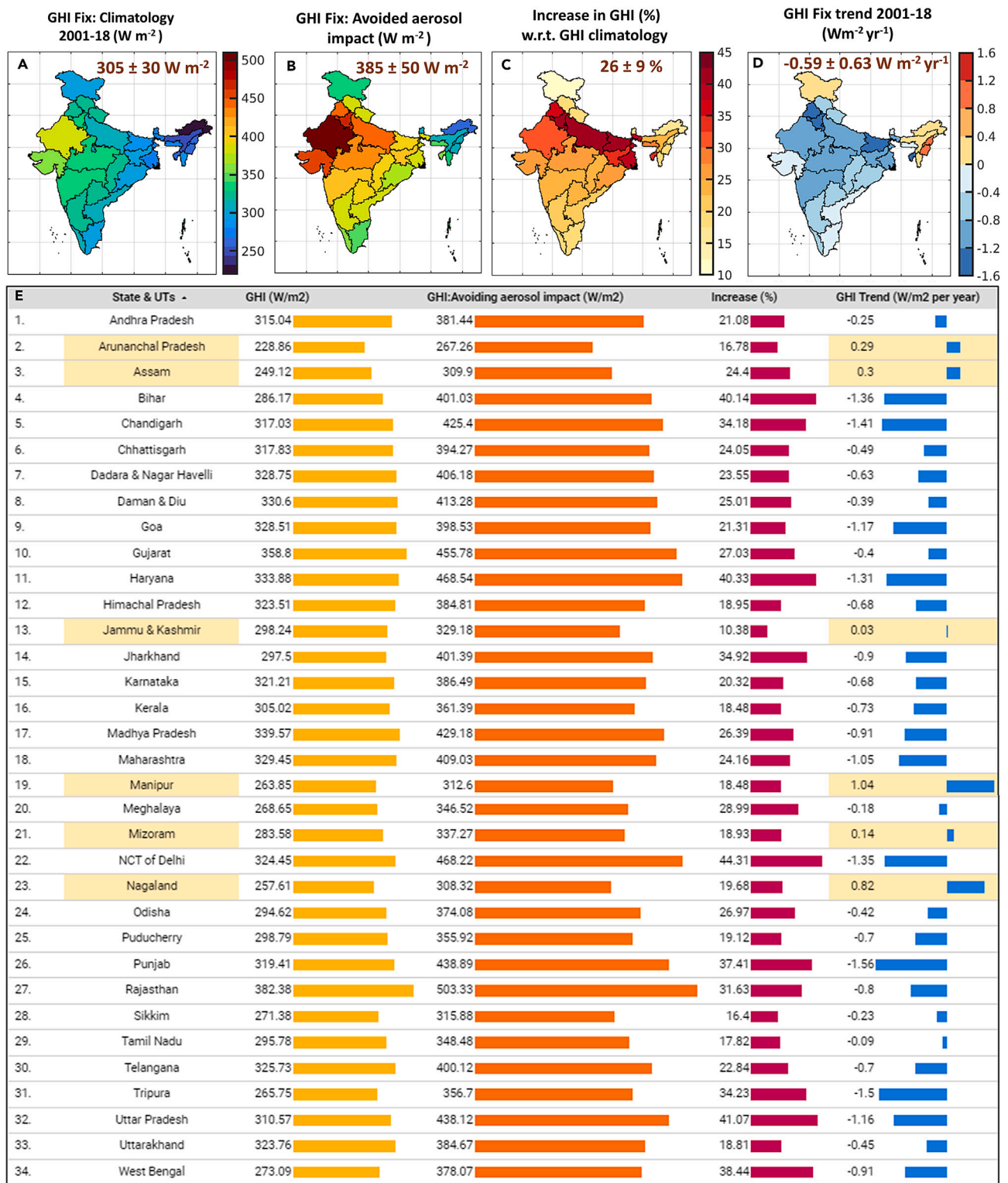 - Solar radiation (SARAH-E) dataset

Figure 6. Indian State and Union Territories (UTs) specific illustration of Global Horizontal Irradiance (GHI) at fixed tilted panels
(A) GHI-Fixed tilted climatology of each state for 2001–18.
(B) GHI-Fixed tilted climatology of each state, avoiding aerosol impact for the period of 2001–18.

Figure 6. *Continued*

(C) Percentage increase in GHI of each state considering avoiding aerosol load and baseline scenario.

(E) Table showing the state-wise statistics. In (E), the states which are experiencing brightening are highlighted with light saffron color. The all-India average is shown in (A–D) in deep brown color.

- ○ Comparison of CERES with SARAH-E data
- ○ Aerosol and cloud impact definitions
- ○ Defining land availability criteria for SPV set-up
- ○ Analysis of solar dimming/brightening on SPV potential and generation
- ○ Analysis for optimally tilted solar panel setting
- ● QUANTIFICATION AND STATISTICAL ANALYSIS

SUPPLEMENTAL INFORMATION

Supplemental information can be found online at https://doi.org/10.1016/j.isci.2023.107856.

AUTHOR CONTRIBUTIONS

S.G.: Conceptualization, Data curation, Investigation, Methodology, Formal analysis, Writing – original draft, review and editing, and Fund acquisition. A.K.: Data curation and Visualization. D.G.: Writing – review and editing, Supervision, Fund acquisition. S.D.: Conceptualization, Methodology, Writing – review and editing, Supervision, and Fund acquisition.

DECLARATION OF INTERESTS

The authors declare no competing interests.

INCLUSION AND DIVERSITY

We support inclusive, diverse, and equitable conduct of research.

REFERENCES

1. IEA PV Snapshot 2020.Pdf (International Energy Agency). https://iea-pvps.org/wp-content/uploads/2020/04/IEA_PVPS_Snapshot_2020.pdf.

2. RENEWABLE CAPACITY STATISTICS 2022. International Renewable Energy Agency. https://en.wikipedia.org/wiki/Solar_power_by_country.

3. Gilgen, H., Wild, M., and Ohmura, A. (1998). Means and trends of shortwave irradiance at the surface estimated from global energy balance archive data. J. Clim. *11*, 2042–2061. https://doi.org/10.1175/1520-0442-11.8.2042.

4. Liepert, B.G. (2002). Observed reductions of surface solar radiation at sites in the United States and worldwide from 1961 to 1990. Geophys. Res. Lett. *29*, 61-1–61-4. https://doi.org/10.1029/2002GL014910.

5. Wild, M., Gilgen, H., Roesch, A., Ohmura, A., Long, C.N., Dutton, E.G., Forgan, B., Kallis, A., Russak, V., and Tsvetkov, A. (2005). From dimming to brightening: Decadal changes in solar radiation at Earth's surface. Science *308*, 847–850. https://doi.org/10.1126/science.1103215.

6. Pinker, R.T., Zhang, B., and Dutton, E.G. (2005). Do satellites detect trends in surface solar radiation? Science *308*, 850–854. https://doi.org/10.1126/science.1103159.

7. Soni, V.K., Pandithurai, G., and Pai, D.S. (2012). Evaluation of long-term changes of solar radiation in India. Int. J. Climatol. *32*, 540–551. https://doi.org/10.1002/joc.2294.

8. Kaiser, D.P., and Qian, Y. (2002). Decreasing trends in sunshine duration over China for 1954–1998: indication of increased haze pollution? Geophys. Res. Lett. *29*, 38–41. https://doi.org/10.1029/2002GL016057.

9. Streets, D.G., Wu, Y., and Chin, M. (2006). Two-decadal aerosol trends as a likely explanation of the global dimming/brightening transition. Geophys. Res. Lett. *33*, L15806. https://doi.org/10.1029/2006GL026471.

10. Norris, J.R., and Wild, M. (2007). Trends in aerosol radiative effects over Europe inferred from observed cloud cover, solar "dimming," and solar "brightening". J. Geophys. Res. *112*, D08214. https://doi.org/10.1029/2006JD007794.

11. Wild, M. (2012). Enlightening global dimming and brightening. Bull. Am. Meteorol. Soc. *93*, 27–37. https://doi.org/10.1175/BAMS-D-11-00074.1.

12. Zhou, Z., Lin, A., Wang, L., Qin, W., Zhao, L., Sun, S., Zhong, Y., He, L., and Chen, F. (2021). Estimation of the losses in potential concentrated solar thermal power electricity

production due to air pollution in China. Sci. Total Environ. *784*, 147214. https://doi.org/10.1016/j.scitotenv.2021.147214.

13. Padma Kumari, B., Londhe, A.L., Daniel, S., and Jadhav, D.B. (2007). Observational evidence of solar dimming: Offsetting surface warming over India. Geophys. Res. Lett. *34*, L21810.

14. NITI Aayog (2015). Report of the Expert Group on 175 GW of RE by 2022 National Institution for Transforming India Government of India. https://smartnet.niua.org/sites/default/files/resources/report-175-GW-RE.pdf.

15. Hernandez, R.R., Hoffacker, M.K., and Field, C.B. (2015). Efficient use of land to meet sustainable energy needs. Nat. Clim. Change *5*, 353–358. https://doi.org/10.1038/nclimate2556.

16. Bhushan, C., Kumarankandath, A., and Goswami, N. (2015). The State of Concentrated Solar Power in India: A Roadmap to Developing Solar Thermal Technologies in India (Centre for Science and Environment). http://citeseerx.ist.psu.edu/viewdoc/download?doi=10.1.1.692.3968&rep=rep1&type=pdf.

17. Van de Ven, D.J., Capellan-Peréz, I., Arto, I., Cazcarro, I., de Castro, C., Patel, P., and Gonzalez-Eguino, M. (2021). The potential land requirements and related land use change emissions of solar energy. Sci. Rep. *11*, 1–12. https://doi.org/10.1038/s41598-021-82042-5.

18. Lopez, A., Roberts, B., Heimiller, D., Blair, N., and Porro, G. (2012). US Renewable Energy Technical Potentials. A GIS-Based Analysis (National Renewable Energy Lab. (NREL)). https://www.nrel.gov/docs/fy12osti/51946.pdf.

19. Doris, E., Lopez, A., and Beckley, D. (2013). Geospatial Analysis of Renewable Energy Technical Potential on Tribal Lands (National Renewable Energy Lab. (NREL)). https://www.nrel.gov/docs/fy13osti/56641.pdf.

20. Saaty, T.L. (2008). Decision making with the analytic hierarchy process. Int. J. Serv. Sci. *1*, 83–98. https://www.rafikulislam.com/uploads/resourses/197245512559a37aadea6d.pdf.

21. Majumdar, D., and Pasqualetti, M.J. (2019). Analysis of land availability for utility-scale power plants and assessment of solar photovoltaic development in the state of Arizona, USA. Renew. Energy *134*, 1213–1231. https://doi.org/10.1016/j.renene.2018.08.064.

22. Aly, A., Jensen, S.S., and Pedersen, A.B. (2017). Solar power potential of Tanzania: Identifying CSP and PV hot spots through a GIS multicriteria decision making analysis. Renew. Energy *113*, 159–175. https://doi.org/10.1016/j.renene.2017.05.077.

23. Yushchenko, A., De Bono, A., Chatenoux, B., Kumar Patel, M., and Ray, N. (2018). GIS-based assessment of photovoltaic (PV) and concentrated solar power (CSP) generation potential in West Africa. Renew. Sustain. Energy Rev. *81*, 2088–2103. https://doi.org/10.1016/j.rser.2017.06.021.

24. Watson, J.J., and Hudson, M.D. (2015). Regional Scale wind farm and solar farm suitability assessment using GIS-assisted multi-criteria evaluation. Landsc. Urban Plann. *138*, 20–31. https://doi.org/10.1016/j.landurbplan.2015.02.001.

25. Al Garni, H.Z., and Awasthi, A. (2017). Solar PV power plant site selection using a GIS-AHP based approach with application in Saudi Arabia. Appl. Energy *206*, 1225–1240. https://doi.org/10.1016/j.apenergy.2017.10.024.

26. Mahtta, R., Joshi, P.K., and Jindal, A.K. (2014). Solar power potential mapping in India using remote sensing inputs and environmental parameters. Renew. Energy *71*, 255–262. https://doi.org/10.1016/j.renene.2014.05.037.

27. Deshmukh, R., Wu, G.C., Callaway, D.S., and Phadke, A. (2019). Geospatial and techno-economic analysis of wind and solar resources in India. Renew. Energy *134*, 947–960. https://doi.org/10.1016/j.renene.2018.11.073.

28. Jain, A., Das, P., Yamujala, S., Bhakar, R., and Mathur, J. (2020). Resource potential and variability assessment of solar and wind energy in India. Energy *211*, 118993. https://doi.org/10.1016/j.energy.2020.118993.

29. Qiu, T., Wang, L., Lu, Y., Zhang, M., Qin, W., Wang, S., and Wang, L. (2022). Potential assessment of photovoltaic power generation in China. Renew. Sustain. Energy Rev. *154*, 111900. https://doi.org/10.1016/j.rser.2021.111900.

30. Müller, B., Wild, M., Driesse, A., and Behrens, K. (2014). Rethinking solar resource assessments in the context of global dimming and brightening. Sol. Energy *99*, 272–282. https://doi.org/10.1016/j.solener.2013.11.013.

31. Li, X., Wagner, F., Peng, W., Yang, J., and Mauzerall, D.L. (2017). Reduction of solar photovoltaic resources due to air pollution in China. Proc. Natl. Acad. Sci. USA *114*, 11867–11872. https://doi.org/10.1073/pnas.1711462114.

32. Bergin, M.H., Ghoroi, C., Dixit, D., Schauer, J.J., and Shindell, D.T. (2017). Large reductions in solar energy production due to dust and particulate air pollution. Environ. Sci. Technol. Lett. *4*, 339–344. https://doi.org/10.1021/acs.estlett.7b00197.

33. Peters, I.M., Karthik, S., Liu, H., Buonassisi, T., and Nobre, A. (2018). Urban haze and photovoltaics. Energy Environ. Sci. *11*, 3043–3054. https://doi.org/10.1039/C8EE01100A.

34. Sweerts, B., Pfenninger, S., Yang, S., Folini, D., Van der Zwaan, B., and Wild, M. (2019). Estimation of losses in solar energy production from air pollution in China since 1960 using surface radiation data. Nat. Energy *4*, 657–663. https://doi.org/10.1038/s41560-019-0412-4.

35. Li, T., Li, X., Meng, H., Chen, L., and Meng, F. (2020). Global reduction of solar power generation efficiency due to aerosols and panel soiling. Int. J. Med. Sci. *17*, 720–727. https://doi.org/10.1038/s41893-020-0553-2.

36. Dumka, U.C., Kosmopoulos, P.G., Ningombam, S.S., and Masoom, A. (2021). Impact of aerosol and cloud on the solar energy potential over the central gangetic himalayan region. Rem. Sens. *13*, 3248. https://doi.org/10.3390/rs13163248.

37. Dumka, U.C., Kosmopoulos, P.G., Patel, P.N., and Sheoran, R. (2022). Can Forest Fires Be an Important Factor in the Reduction in Solar Power Production in India? Rem. Sens. *14*, 549. https://doi.org/10.3390/rs14030549.

38. Ghosh, S., Dey, S., Ganguly, D., Baidya Roy, S., and Bali, K. (2022). Cleaner air would enhance India's annual solar energy production by 6–28 TWh. Environ. Res. Lett. *17*, 054007. https://doi.org/10.1088/1748-9326/ac5d9a.

39. Soni, V.K., Pandithurai, G., and Pai, D.S. (2016). Is there a transition of solar radiation from dimming to brightening over India?

Atmos. Res. *169*, 209–224. https://doi.org/10.1016/j.atmosres.2015.10.010.

40. CERES Science Team (2017). CERES SYN1deg Ed4A data quality summary, dataset user guide. https://ceres.larc.nasa.gov/data/.

41. Didan, K.. MOD13C2 MODIS/Terra Vegetation Indices Monthly L3 Global 0.05 Deg CMG V006, 2015, distributed by NASA EOSDIS Land Processes DAAC, dataset user guide. https://vip.arizona.edu/documents/MODIS/MODIS_VI_UsersGuide_June_2015_C6.pdf.

42. Dijkstra, L., and Poelmann, H.. A harmonized definition of cities and rural areas: The new degree of urbanization. Eur. Comm. Urban Reg. Pol.2014, dataset user guide. https://ec.europa.eu/regional_policy/sources/docgener/work/2014_01_new_urban.pdf.

43. Muneer, T., Asif, M., and Munawwar, S. (2005). Sustainable production of solar electricity with particular reference to the Indian economy. Renew. Sustain. Energy Rev. *9*, 444–473. https://doi.org/10.1016/j.rser.2004.03.004.

44. Solar. Ministry of New and Renewable Energy, Govt. of India. https://web.archive.org/web/20140225160014/http://www.mnre.gov.in/schemes/grid-connected/solar/.

45. Dey, S., and Di Girolamo, L. (2010). A climatology of aerosol optical and microphysical properties over the Indian subcontinent from 9 years (2000–2008) of Multiangle Imaging Spectroradiometer (MISR) data. J. Geophys. Res. *115*, D15204. https://doi.org/10.1029/2009JD013395.

46. Lau, W.K., Kim, K.M., Hsu, C.N., and Holben, B.N. (2009). Possible influences of air pollution, dust-and sandstorms on the Indian monsoon. World Meteorol. Organ. Bull. *58*, 22. https://public.wmo.int/en/bulletin/possible-influences-air-pollution-dust-and-sandstorms-indian-monsoon.

47. Venkataraman, C., Habib, G., Kadamba, D., Shrivastava, M., Leon, J.F., Crouzille, B., Boucher, O., and Streets, D.G. (2006). Emissions from open biomass burning in India: Integrating the inventory approach with high-resolution Moderate Resolution Imaging Spectroradiometer (MODIS) active-fire and land cover data. Global Biogeochem. Cycles *20*. https://doi.org/10.1029/2005GB002547.

48. Gelaro, R., McCarty, W., Suárez, M.J., Todling, R., Molod, A., Takacs, L., Randles, C.A., Darmenov, A., Bosilovich, M.G., Reichle, R., and Wargan, K. (2017). The modern-era retrospective analysis for research and applications, version 2 (MERRA-2). J. Clim. *30*, 5419–5454. https://doi.org/10.1175/JCLI-D-16-0758.1.

49. Randles, C.A., Da Silva, A.M., Buchard, V., Colarco, P.R., Darmenov, A., Govindaraju, R., Smirnov, A., Holben, B., Ferrare, R., Hair, J., et al. (2017). The MERRA-2 aerosol reanalysis, 1980 onward. Part I: System description and data assimilation evaluation. J. Clim. *30*, 6823–6850. https://doi.org/10.1175/JCLI-D-16-0609.1.

50. Pandey, S.K., Vinoj, V., Landu, K., and Babu, S.S. (2017). Declining pre-monsoon dust loading over South Asia: Signature of a changing regional climate. Sci. Rep. *7*, 16062–16110. https://doi.org/10.1038/s41598-017-16338-w.

51. Ramachandra, T.V., Jain, R., and Krishnadas, G. (2011). Hotspots of solar potential in India. Renew. Sustain. Energy Rev. *15*, 3178–3186. https://doi.org/10.1016/j.rser.2011.04.007.

52. India State-Level Disease Burden Initiative Air Pollution Collaborators, Dey, S., Gupta, T., Dhaliwal, R.S., Brauer, M., Cohen, A.J., and Dandona, L. (2019). The impact of air pollution on deaths, disease burden, and life expectancy across the states of India: the Global Burden of Disease Study 2017. Lancet Planet. Health 3, e26–e39.

53. Christensen, M.W., Jones, W.K., and Stier, P. (2020). Aerosols enhance cloud lifetime and brightness along the stratus-to-cumulus transition. Proc. Natl. Acad. Sci. USA 117, 17591–17598. https://doi.org/10.1073/pnas.1921231117.

54. Twomey, S. (1974). Pollution and the planetary albedo. Atmos. Environ. 8, 1251–1256. https://doi.org/10.1016/0004-6981(74)90004-3.

55. Doelling, D.R., Loeb, N.G., Keyes, D.F., Nordeen, M.L., Morstad, D., Nguyen, C., Wielicki, B.A., Young, D.F., and Sun, M. (2013). Geostationary enhanced temporal interpolation for CERES flux products. J. Atmos. Ocean. Technol. 30, 1072–1090. https://doi.org/10.1175/JTECH-D-12-00136.1.

56. Doelling, D.R., Sun, M., Nguyen, L.T., Nordeen, M.L., Haney, C.O., Keyes, D.F., and Mlynczak, P.E. (2016). Advances in geostationary-derived longwave fluxes for the CERES synoptic (SYN1deg) product. J. Atmos. Ocean. Technol. 33, 503–521. https://doi.org/10.1175/JTECH-D-15-0147.1.

57. Rutan, D.A., Kato, S., Doelling, D.R., Rose, F.G., Nguyen, L.T., Caldwell, T.E., and Loeb, N.G. (2015). CERES synoptic product: Methodology and validation of surface radiant flux. J. Atmos. Ocean. Technol. 32, 1121–1143. https://doi.org/10.1175/JTECH-D-14-00165.1.

58. Platnick, S., Hubanks, P., Meyer, K., and King, M.D. (2015). MODIS Atmosphere L3 Monthly Product (08_L3). NASA MODIS Adaptive Processing System, Goddard Space Flight Cente. https://doi.org/10.5067/MODIS/MOD08_M3.061.

59. ISCCP definition of cloud types. https://isccp.giss.nasa.gov/cloudtypes.html.

60. Amillo, A., Huld, T., and Müller, R. (2014). A new database of global and direct solar radiation using the eastern meteosat satellite, models, and validation. Rem. Sens. 6, 8165–8189. https://doi.org/10.3390/rs6098165.

61. Huld, T., Müller, R., Gracia-Amillo, A., Pfeifroth, U., and Trentmann, J. (2016). Surface Solar Radiation Data Set—Heliosat. Meteosat-East (SARAH-E), Dataset. https://doi.org/10.5676/DWD/JECD/SARAH_E/V001.

62. Beyer, H.G., Costanzo, C., and Heinemann, D. (1996). Modifications of the Heliosat procedure for irradiance estimates from satellite images. Sol. Energy 56, 207–212. https://doi.org/10.1016/0038-092X(95)00092-6.

63. Krämer, M., Müller, R., Bovensmann, H., Burrows, J., Brinkmann, J., Röth, E.P., Grooß, J.-U., Müller, R., Woyke, T., Ruhnke, R., and Günther, G. (2003). Intercomparison of stratospheric chemistry models under polar vortex conditions. J. Atmos. Chem. 45, 51–77. https://doi.org/10.1023/A:1024056026432.

64. Mayer, B., and Kylling, A. (2005). The libRadtran software package for radiative transfer calculations-description and examples of use. Atmos. Chem. Phys. 5, 1855–1877. https://doi.org/10.5194/acp-5-1855-2005.

65. SARAH-E, Product User Manual (PUM). https://www.cmsaf.eu/SharedDocs/Literatur/document/2017/saf_cm_dwd_pum_sarah_e_1_0_1_pdf.pdf?__blob=publicationFile.

66. Riihelä, A., Kallio, V., Devraj, S., Sharma, A., and Lindfors, A. (2018). Validation of the Sarah-e satellite-based surface solar radiation estimates over India. Rem. Sens. 10, 392. https://doi.org/10.3390/rs10030392.

67. Inamdar, A., and Guillevic, P. (2015). Net surface shortwave radiation from GOES imagery—Product evaluation using ground-based measurements from SURFRAD. Rem. Sens. 7, 10788–10814. https://doi.org/10.3390/rs70810788.

68. Ma, Y., Zhang, Y., Liang, X., Oglesbee, M., Krakowka, S., Niehaus, A., Wang, G., Jia, A., Song, H., and Li, J. (2016). Validation and spatiotemporal analysis of CERES surface net radiation product. Vet. Microbiol. 186, 90–96. https://doi.org/10.3390/rs8020090.

69. Yang, S., Zhou, Z., Yu, Y., and Wild, M. (2021). Cloud 'shrinking' and 'optical thinning' in the 'dimming' period and a subsequent recovery in the 'brightening' period over China. Environ. Res. Lett. 16, 034013. https://doi.org/10.1088/1748-9326/abdf89.

70. Akbar, T.A., Hassan, Q.K., Ishaq, S., Batool, M., Butt, H.J., and Jabbar, H. (2019). Investigative spatial distribution and modelling of existing and future urban land changes and its impact on urbanization and economy. Rem. Sens. 11, 105. https://doi.org/10.3390/rs11020105.

STAR★METHODS

KEY RESOURCES TABLE

REAGENT or RESOURCE	SOURCE	IDENTIFIER
Deposited data		
Radiation products: CERES[40] synoptic gridded (SYN1deg) version 4.1	NASA CERES	https://ceres.larc.nasa.gov/data/
MODIS Normalized Difference Vegetation Index (NDVI) level-3 version 6 monthly gridded dataset for the year 2018 at 0.05° climate modeling grid (MOD13C2)[41]	LAADS DAAC NASA	https://ladsweb.modaps.eosdis.nasa.gov/missions-and-measurements/products/MOD13C2
Global Human Settlement Layer (GHSL) 42	European Commission	https://ghsl.jrc.ec.europa.eu/dataToolsOverview.php
Cloud and its characteristics: Moderate Resolution Imaging Spectroradiometer (MODIS-Terra) level-3 atmosphere gridded product (MOD08 D3 v6.1)[58]	LAADS DAAC NASA	https://ladsweb.modaps.eosdis.nasa.gov/missions-and-measurements/products/MOD08_M3
Cloud classifications: International Satellite Cloud Climatology Project (ISCCP)[59]	NASA	https://isccp.giss.nasa.gov/cloudtypes.html
Solar installation capacity and generation data for the FY 2019-20	Central Electricity Authority, Ministry of Power (CEA, MoP, Government of India)	http://cea.nic.in/monthlyarchive.html
Solar Parks, National Solar Schemes, Solar City	Ministry of New and Renewable Energy, (MNRE, Government of India)	https://www.yellowhaze.in/list-of-solar-parks-in-india/ https://mnre.gov.in/solar/schemes https://pib.gov.in/newsite/Printrelease.aspx?relid=123606
Surface Solar Radiation DataSet - Heliosat Meteosat-East (SARAH-E),[60–62] Edition 1	Satellite Application Facility on Climate Monitoring (CM SAF), EUMETSAT	https://wui.cmsaf.eu/safira/action/viewProduktSearch
Software and algorithms		
MATLAB R2020b	MathWorks	https://in.mathworks.com/products/matlab.html
Google Data Studio	Google	https://datastudio.withgoogle.com/
Code to reproduce the results of this study	Authors (This study)	https://github.com/Sushovan-453?tab=repositories

RESOURCE AVAILABILITY

Lead contact

Further information for data and code files should be directed to and will be provided by the lead contact, Sushovan Ghosh (Sushovan.Ghosh@cas.iitd.ac.in).

Materials availability

This study did not generate new datasets.

Data and code availability

- This paper analyzes existing, publicly available data. These accession numbers for the datasets are listed in the key resources table.
- All original code has been deposited on Github and is publicly available. Links are listed in the key resources table.
- Any additional information required to reanalyze the data reported in this paper is available from the lead contact upon request.

METHOD DETAILS

Solar radiation datasets

We process synoptic gridded (SYN1deg) version 4.1 daily data from CERES of downward shortwave (0.3–5 μm) flux. The analysis is done from 2001 to 2018 (18 years of data). We use NASA CERES-SYN1deg monthly surface direct, diffuse radiation, and Aerosol Optical Depth (AOD) at 550 nm at a horizontal resolution of 1° latitude ✕ 1° longitude. These data products are computed using the Langley Fu–Liou radiative transfer

model, and the calculations are constrained by the various input data such as aerosol, cloud, and atmospheric conditions (e.g., the profile of temperature, pressure, water vapor, ozone, etc.) data. The details are stated in Rutan et al. 2015 and Doelling et al. 2013, 2016.[55–57] It also provides computed surface, and profile radiant fluxes at different atmospheric states such as clear-sky (CS, including aerosol, no clouds), all-sky-no-aerosol (NAER, 'no aerosol,' include clouds), and all-sky (AS, which consists of both aerosol and cloud, a better representation of the real atmosphere) conditions with inputs described earlier. These different radiation products are previously used to estimate the aerosol and cloud impact on solar energy generations.[31,35,38]

Cloud datasets

We use Moderate Resolution Imaging Spectroradiometer (MODIS-Terra) level-3 atmosphere gridded product (MOD08 D3 v6.1)[58] for cloud fraction and cloud top pressure at a daily scale for our analysis. Our study follows the International Satellite Cloud Climatology Project [ISCCP] classification for determining the low-level (below 680 hPa), mid-level (above 680 hPa but below 440 hPa), and high-level (above 440 hPa) clouds.[59] A varied range of statistical summaries (such as mean, standard deviation, maximum, minimum, and identification of clear/cloudy pixel) have been computed into 1 ° × 1° grid cells depending on the parameters to be in consideration. MODIS science team maintains rigorous quality assurance, calibration, and validation processes. This includes the inter-comparisons of MODIS data with various data from other satellites, airborne, surface, and *in situ* measurements. More details about the product information and validation are depicted in Platnick et al., 2015.[58]

NDVI and GHSL datasets

We use MODIS Normalized Difference Vegetation Index (NDVI) level-3 version 6 monthly gridded dataset for the year 2018 at 0.05° climate modeling grid (MOD13C2).[41] MODIS NDVI is produced at 16-day intervals and considered as a continuity index to the existing National Oceanic and Atmospheric Administration-Advanced Very High-Resolution Radiometer (NOAA-AVHRR) derived NDVI. This has been calculated based on atmospherically corrected reflectance from the red and near-infrared wavelengths and bears a valid range between −1 and 1. The vegetation index values are available on a per-pixel basis and have been generated through a weighted temporal average from the MOD13A2 product. More details of the quality flag and other technical descriptions are stated by Didan et al., 2015.[41] Along with the NDVI, we use the Global Human Settlement Layer (GHSL)[42] data from the European Commission to identify the appropriate site for setting up the SPV system. The GHSL project provides spatial information at a global scale through evidence-based analytics and knowledge of human occupancy. It has been generated by tracking the 40-year of Landsat imagery that produces land-use and land-cover changes along with the other geospatial information linked with human presence. We use GHS-Settlement Model grid (GHS-SMOD) data for the years 1975, 1990, 2001, and 2015. In this dataset, based on the above information, each 1-km × 1-km grid is assigned to one of the four classes – high-density-urban (population density ≥ 1500 km^{-2}), low-density-urban ($300 \leq$ population density ≥ 1500 km^{-2}), rural (population density ≤ 300 km^{-2}) and no-settlement grid (no permanent human habitation). We use the latest GHSL data (for 2015) to identify land availability criteria for further expansion of solar resources in India.

Solar energy capacity and generation datasets

We use the available solar installation capacity and generation data for the FY 2019-20 from Central Electricity Authority, Ministry of Power (CEA, MoP, Government of India). The data is available at http://cea.nic.in/monthlyarchive.html.

Solar radiation (SARAH-E) dataset

The Surface Solar Radiation DataSet - Heliosat Meteosat-East (SARAH-E), Edition 1 is produced by the Satellite Application Facility on Climate Monitoring (CM SAF) Collaboration based on observations from the Meteosat Visible Infra-Red Imager (MVIRI) instruments onboard the Meteosat First Generation (MFG) is known as SARAH-East. It provides 18 years of (1999–2016) climate data records of solar surface irradiance, the surface direct irradiance, and the direct normalized irradiance at a spatial resolution of 0.05° (within 70°N-S,10°W-130°E).[60,61] The retrieval algorithm is based on the Heliostat method, which assumes that all solar radiation encountering the Earth's atmosphere will either be reflected away by the cloud or penetrate through it to reach the surface as solar irradiance. This method is completely based on image counts, based on which cloud albedo has been computed.[62] Based on the different inputs such as water vapor from ERA-interim Reanalysis, ozone content of the Max-Planck institute of air chemistry,[63] a look-up table (LUT) generated from the Radiative Transfer Model (RTM) libRadtran[64] and the surface albedo from Surface and Atmospheric Radiation Budget (SARB)/CERES. The detailed descriptions are documented in the product user manual.[65] The SARAH-E has been validated against India Meteorological Data recently.[66]

Comparison of CERES with SARAH-E data

We compare CERES data with the Surface Solar Radiation Dataset-Heliosat Meteosat-East (SARAH-E), Edition 1 over the Indian region for a 16-year (2001-16) tenure. The spatial trends from both datasets are well in agreement. Most of the broader patterns are captured well. Additionally, the spatial correlation and the point correlation show a high level of concurrence. The statistics are shown in Figure S16. The discrepancy in spatial trends between CERES and SARAH-E over Jammu and Kashmir and Ladakh may be due to inherent inconsistency in retrieval over snow-covered regions.[67,68] CERES data has also been evaluated against various ground station data globally.[40] Recently, it has been evaluated over the Indian region with the three prominent ground datasets and found suitable for solar resource assessment study.[38]

Aerosol and cloud impact definitions

The aerosol and cloud attribution in obscuring the radiation is computed using the following relations: Direct aerosol impact = (NAER −AS); Cloud impact = (CS −AS). The details of the various radiation products are depicted in Table S1, and the complete flowchart of our research plan is presented in Figure S17. The amount of radiation exposure over the latitudinally fixed-tilted solar panel (known as optimally tilted panel configuration) is calculated based on Ghosh et al., 2022[38] and is not repeated here. Based on the earlier study,[69] we define AOD-induced-aerosol-impact by taking the ratio of aerosol-impact and exponential of AOD and cloud fraction-induced-cloud-impact by taking the ratio of cloud-impact and the exponential of cloud fraction. The exponential of AOD and cloud fraction in defining the above terms give better statistics as compared to linear relationships and agree with the Beer-Lambert law in AOD-radiation interaction. These terms give the optical effectiveness of per unit change of the controlling factors (i.e., aerosol loading and cloud fractions) in blocking the radiation from reaching the surface.

Defining land availability criteria for SPV set-up

The technology for harnessing solar energy at a utility scale requires adequate land and constraints by several factors such as terrain type, the protected status of the land, eco-system, wildlife preservations, and, most importantly, human settlements. Keeping this in mind, we choose no-settlement-layer grids from the GHSL data and overlay the NDVI with the range of 0.07<NDVI≤0.4. Within this NDVI range, we include built-up, barren, shrub, grassland, and very sparse vegetation, and NDVI below 0.07 mostly are water bodies, mountains, and NDVI greater than 0.4 are dense vegetation (mostly forestry and agricultural land).[70] Most of the existing and commissioned solar parks [Available at: https://www.yellowhaze.in/list-of-solar-parks-in-india/; Solar Scheme, Ministry of New and Renewable Energy, Government of India. Available at: https://mnre.gov.in/solar/schemes] in India are located over these identified land areas (see Figure S10; Table S4). This makes our probable land identification well-suited for utility-scale SPV set-up in India (and broadly elsewhere). Furthermore, we combine rural, low-density-urban, and high-density-urban grids from GHSL data for rooftop installation set-up. This consideration supports the Government of India's (GoI's) initiatives to provide clean and affordable energy to Indian rural livelihood and promotes the "Green-city" [Available at: https://pib.gov.in/newsite/Printrelease.aspx?relid=123606] endeavors (Table S5). This establishes the overall credibility of our landmass criteria for the solar expansion exercises in India. Using the nearest-neighbor algorithm, we extract statistics of direct and diffuse radiation at the identified land-use grid points[Available:https://pro.arcgis.com/en/pro-app/2.8/tool-reference/data-management/resample.htm].

Analysis of solar dimming/brightening on SPV potential and generation

We find that 29.3% of total available Indian landmass exposed to at least 5 kWhm^{-2}d^{-1} of radiation (spreads over barren, shrubland, desert, and other wastelands) has been declining at 0.21% y^{-1} during the last 18-year (2001-18). The Total Geographical Area of India is ∼3.287 million km.^{2} So, this 0.21% SPV area is translated to 6902 km^2 of potential area which is probable to have 50 GW of SPV potential considering the land use factor of 7.5 MW km^{-2} area27. Typically, a 1 MW plant can produce 1.44 GWh of solar power on an annual basis [CleanMax Powering Sustainability, (https://www.cleanmax.com/knowledge-hub/faq.php#:∼:text=How%20much%20electricity%20will%20be,of%20the%20solar%20power%20plant; WAAREE, One with the sun, https://www.waaree.com/blog/1mw-solar-power-plant-generate-electricity in month#:∼:text = Electricity%20Generated%20by%201MW%20Solar,the%20help%20of%20an%20example). Therefore, 50 GW can potentially produce 75 TWh (=50 × 1.44) solar power per year.

Analysis for optimally tilted solar panel setting

Estimation of solar radiation over the latitudinally fixed-tilted panel configuration (also known as optimally tilted panel) consider beam (I_B), diffuse (I_D) and reflected radiation (I_R) (from the surrounding surfaces). The total radiation (I_T) impinges on the tilted panel is given by: $I_T = I_B + I_D + I_R$. The calculation is based on the formula used in Ghosh et al., 2022 (in supplementary section (II.1)) and is not repeated here.[38] The annual average exposed radiation on ideally tilted fixed solar panel surfaces is 305 ± 30 Wm^{-2} (∼1.5 times more w.r.t. horizontal flat surface configurations) but declining at a rate of −0.59 ± 0.63 Wm^{-2}y^{-1} (∼twice w.r.t. horizontal flat surface settings) which is equivalent to ∼0.20% of the annual mean exposed radiation. This translates to a loss of ∼100 GWh of generation annually (considering India's annual solar power generation of 50 TWh till 2019-20), equivalent to ∼5 million USD (considering INR 3.85 kWh^{-1} (∼0.052 USD kWh^{-1}) of consumption [CERC 2021 Calculation of average power purchase cost (APPC) rate at the national level, Petition No. 01/SM/2021 (New Delhi: Central Electricity Regulatory Commission, Government of India) available at: https://cercind.gov.in/2021/orders/01-SM-2021.pdf].

QUANTIFICATION AND STATISTICAL ANALYSIS

The all sorts of statistical measure such as mean, standard deviation, linear least-square trend and statistical significance tests are carried out using MATLAB 2020b. All original code has been deposited on Github and is publicly available. Links are listed in the key resources table.

Details of linear least-square trends, statistical significance and stipple functions are available at http://www.chadagreene.com/CDT/CDT_Contents.html.